

Anodic Electrochemistry of Free and Coordinated 1,1'-Bis(di-tert-butylphosphino)ferrocene

Fawn N. Blanco,[†] Laura E. Hagopian,[†] William R. McNamara,[†] James A. Golen,^{‡,§}
Arnold L. Rheingold,[‡] and Chip Nataro^{*,†}

Department of Chemistry, Lafayette College, Easton, Pennsylvania 18042, and Department of Chemistry and Biochemistry, University of California—San Diego, La Jolla, California 92093

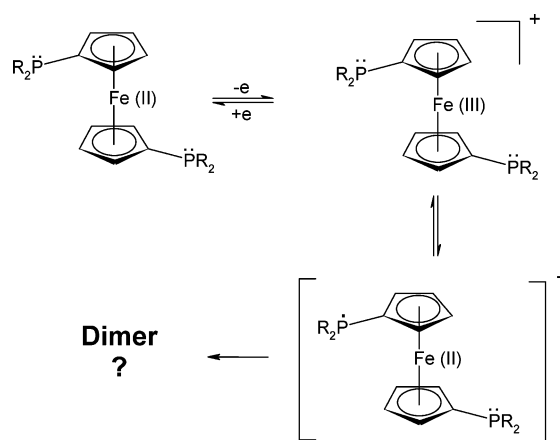
Received November 23, 2005

The electrochemistry of 1,1'-bis(di-tert-butylphosphino)ferrocene (dtbpf) was examined in methylene chloride with tetrabutylammonium hexafluorophosphate as the supporting electrolyte. Two new complexes in which dtbpf was bound to a transition metal were prepared and characterized. The two new complexes as well as two previously reported complexes were analyzed by cyclic voltammetry. In addition, the chalcogenides, dtbpfS₂ and dtbpfSe₂, were prepared and characterized by NMR and the structure of dtbpfSe₂ was determined. The oxidation of dtbpfS₂ is a simple one-electron process due to the presence of the iron center. In contrast, the oxidation of dtbpfSe₂ is electrochemically irreversible and appears to proceed by an EE mechanism. Chemical oxidation of dtbpfSe₂ resulted in the formation of [dtbpfSe₂][BF₄]₂, in which a Se–Se bond formed. This compound was characterized by ³¹P NMR and X-ray crystallography. A detailed analysis of the electrochemistry suggests that the oxidation of dtbpfSe₂ occurs by two separate one-electron processes. In addition, formation of the Se–Se bond was reversible.

Introduction

Bis-phosphinometallobenes have received considerable attention in recent years, particularly as ligands in catalytic systems.¹ Our interest has focused on the anodic electrochemistry of these compounds, in particular, how the electrochemistry is affected by changing the substituents on phosphorus. The anodic electrochemistries of 1,1'-bis(diphenylphosphino)ferrocene (dppf)² and 1,1'-bis(di-isopropylphosphino)ferrocene (dippf)³ are complicated by a follow-up reaction, which has been proposed to be dimerization (Scheme 1).⁴ This dimerization can be affected by changing the electrochemical conditions (lower concentrations of bis-phosphinometallobene or higher scan rates) and/or changing the groups on the phosphorus atoms. The rates of the follow-up reactions indicate that the proposed dimerization of dppf⁺ is less favorable than that of dippf⁺.^{2,3} On the basis of a steric argument, it would be expected that the dppf⁺ reaction would be less likely to occur since the isopropyl groups are bulkier than phenyl groups.⁵ However, electronic arguments

Scheme 1. Proposed Dimerization Reaction of 1,1'-Bis(diphosphino)ferrocenes



suggest that the phenyl groups can stabilize the phosphorus radical cation by delocalizing it into the π -system, thereby making the dimerization less favorable. Because dippf⁺ dimerization occurs at a higher rate, it would suggest that electronic effects are more important than steric effects.^{2,3}

Since the dimerization of the oxidized form of these bis-phosphinometallobenes is proposed to occur through a phosphorus atom, examining the electrochemistry of compounds in which the lone pair on phosphorus is occupied is of interest. Occupying the lone pair can be accomplished by coordinating the phosphorus atoms to a Lewis acid or by forming the phosphine chalcogenide (R₃P=E, where E = O, S, or Se). In general, coordination of dppf or dippf to a Lewis acid (e.g., dppf(BH₃)₂ and PtCl₂(dppf)) yields compounds that display an oxidation that is both chemically and electrochemically reversible.^{2,3,6,7} However, there are numerous examples, such as

(5) Liu, H. Y.; Eriks, K.; Prock, A.; Giering, W. P. *Organometallics* 1990, 9, 1758.

* To whom correspondence should be addressed. E-mail: nataroc@lafayette.edu.

[†] Lafayette College.

[‡] University of California—San Diego.

[§] Permanent address: Department of Chemistry and Biochemistry, University of Massachusetts—Dartmouth, North Dartmouth, MA 02747.

(1) The number of publications containing symmetric bis-phosphinometallobenes is quite large. Representative examples from 2006 include: (a) Patil, N. T.; Huo, Z.; Yamamoto, Y. *J. Org. Chem.* 2006, 71, 2503. (b) Trost, B. M.; Richardson, J.; Yong, K. *J. Am. Chem. Soc.* 2006, 128, 2540. (c) Johns, A. M.; Utsunomiya, M.; Incarvito, C. D.; Hartwig, J. F. *J. Am. Chem. Soc.* 2006, 128, 1828. (d) Dhondi, P. K.; Chisholm, J. D. *Org. Lett.* 2006, 8, 67. (e) Boyle, K. L.; Lipsky, E. B.; Kalberg, C. S. *Tetrahedron Lett.* 2006, 47, 1311. (f) Murata, M.; Yoshida, S.; Nirei, S.-I.; Watanabe, S.; Masuda, Y. *Synlett.* 2006, 118. (g) Teo, S.; Weng, Z.; Hor, T. S. *A. Organometallics* 2006, 25, 1199.

(2) Nataro, C.; Campbell, A. N.; Ferguson, M. A.; Incarvito, C. D.; Rheingold, A. L. *J. Organomet. Chem.* 2003, 673, 47, and references therein.

(3) Ong, J. H. L.; Nataro, C.; Golen, J. A.; Rheingold, A. L. *Organometallics* 2003, 22, 5027.

(4) Pilloni, G.; Longato, B.; Corain, B. *J. Organomet. Chem.* 1991, 420, 57.

Chart 1. Bis(phosphino)ferrocenes and Bis(phosphinechalcogenide)ferrocenes Mentioned in This Report

Bis(phosphino)ferrocene		Bis(phosphinechalcogenide)ferrocene			
Abbreviation	R	Abbreviation	R	E ₁	E ₂
dppf	Ph	dppfS ₂	Ph	S	S
dippf	iPr	dppfSe ₂	Ph	Se	Se
dtbpf	tBu	dppfOSe	Ph	O	Se
		dippfS ₂	iPr	S	S
		dippfSe ₂	iPr	Se	Se
		dtbpfS ₂	tBu	S	S
		dtbpfSe ₂	tBu	Se	Se

[NiCl₂(P⁺P)] (P⁺P = dppf or dippf),^{2,3} in which the oxidation is chemically irreversible. Similarly, oxidation of the phosphine chalcogenides tends to be chemically and electrochemically reversible, although oxidation of the phosphine selenides (e.g., dppfSe₂ or dppfOSe) gave what was previously described by this laboratory as an irreversible anodic wave and a cathodic wave due to a follow-up product.⁶

To further investigate the role of electronics and sterics on the oxidative electrochemistry of bis-phosphinometallocenes, we have chosen to examine 1,1'-bis(di-tert-butylpropylphosphino)ferrocene (dtbpf). To date, most of the work with dtbpf has been focused on catalytic systems in which dtbpf is a ligand for the palladium catalyst.⁸ Additional catalytic studies using rhodium and platinum complexes containing dtbpf have also been reported.⁹ Surprisingly, there have not been any investigations into the electrochemistry of dtbpf or complexes containing dtbpf. In this report, we examine the anodic electrochemistry of dtbpf and complexes containing dtbpf as a ligand. In addition, the synthesis and electrochemistry of two dtbpf chalcogenide compounds are presented (Chart 1). The oxidative electrochemistry of the selenide has been closely examined and is now

(6) Swartz, B. D.; Nataro, C. *Organometallics* **2005**, *24*, 2447.

(7) Ohs, A. C.; Rheingold, A. L.; Shaw, M. J.; Nataro, C. *Organometallics* **2004**, *23*, 4655.

(8) (a) Wu, L.; Hartwig, J. F. *J. Am. Chem. Soc.* **2005**, *127*, 15824. (b) Itoh, T.; Mase, T. *Tetrahedron Lett.* **2005**, *46*, 3573. (c) Colacot, T. J.; Shea, H. A. *Org. Lett.* **2004**, *6*, 3731. (d) Dubbaka, S. R.; Vogel, P. *Org. Lett.* **2004**, *6*, 95. (e) Shen, M.; Li, G.; Lu, B. Z.; Hossain, A.; Roschinger, F.; Farina, V.; Senanayake, C. H. *Org. Lett.* **2004**, *6*, 4129. (f) Itoh, T.; Sato, K.; Mase, T. *Adv. Synth., Catal.* **2004**, *346*, 1859. (g) Mann, G.; Shelby, Q.; Roy, A. H.; Hartwig, J. F. *Organometallics* **2003**, *22*, 2775. (h) Fillion, E.; Taylor, N. J. *J. Am. Chem. Soc.* **2003**, *125*, 12700. (i) Mann, G.; Shelby, Q.; Roy, A. H.; Hartwig, J. F. *Organometallics* **2003**, *22*, 2775. (j) van Leeuwen, P. W. N. M.; Zuideveld, M. A.; Swennenhuis, B. H. G.; Freixa, Z.; Kamer, P. C. J.; Goubitz, K.; Fraanje, J.; Lutz, M.; Spek, A. L. *J. Am. Chem. Soc.* **2003**, *125*, 5523. (k) Beare, N. A.; Hartwig, J. F. *J. Org. Chem.* **2002**, *67*, 541. (l) Zuideveld, M. A.; Swennenhuis, B. H. G.; Boele, M. D. K.; Guari, Y.; van Strijdonck, G. P. F.; Reek, J. N. H.; Kamer, P. C. J.; Goubitz, K.; Fraanje, J.; Lutz, M.; Spek, A. L.; van Leeuwen, P. W. N. M. *J. Chem. Soc., Dalton Trans.* **2002**, 2308. (m) Zuideveld, M. A.; Swennenhuis, B. H. G.; Kamer, P. C. J.; van Leeuwen, P. W. N. M. *J. Organomet. Chem.* **2001**, *637*–639, 805. (n) Watanabe, M.; Yamamoto, T.; Nishiyama, M. *Angew. Chem., Int. Ed.* **2000**, *39*, 2501. (o) Mann, G.; Incarvito, C.; Rheingold, A. L.; Hartwig, J. F. *J. Am. Chem. Soc.* **1999**, *121*, 3224. (p) Kawatsura, M.; Hartwig, J. F. *J. Am. Chem. Soc.* **1999**, *121*, 1473.

(9) (a) Muñoz, M. P.; Adrio, J.; Carretero, J. C.; Echavarrén, A. M. *Organometallics* **2005**, *24*, 1293. (b) Kim, T. J. *Bull. Kor. Chem. Soc.* **1990**, *11*, 134. (c) Butler, I. R.; Cullen, W. R.; Kim, T. J.; Rettig, S. J.; Trotter, J. *Organometallics* **1985**, *4*, 972. (d) Cullen, W. R.; Kim, T. J.; Einstein, F. W. B.; Jones, T. *Organometallics* **1985**, *4*, 346. (e) Butler, I. R.; Cullen, W. R.; Kim, T. J.; Einstein, F. W. B.; Jones, T. *J. Chem. Soc., Chem. Commun.* **1984**, 710. (f) Cullen, W. R.; Kim, T. J.; Einstein, F. W. B.; Jones, T. *Organometallics* **1983**, *2*, 714.

thought to consist of a chemically reversible, electrochemically irreversible two-electron process in which there is formation and breaking of a Se–Se bond.

Experimental Section

General Procedures. All reactions were carried out using standard Schlenk techniques under an atmosphere of argon with the exception of the synthesis and manipulations of [dtbpfSe₂][BF₄]₂, which were carried out in a glovebox under an argon atmosphere. Decamethylferrocene (Fc*), selenium, 2,2'-thiodiethanol, and P(tBu)₂(2-biphenyl) were purchased from Aldrich Chemical Co., Inc. and used without additional purification. Sulfur was obtained from Fisher Chemicals, Inc. Acetylferrocene, ferrocene (FcH), [PdCl₂(MeCN)₂], [PtCl₂(C₆H₅CN)₂], HAuCl₄·H₂O, and dtbpf were purchased from Strem Chemicals, Inc. FcH was sublimed prior to use. Acetylferrocenium tetrafluoroborate,¹⁰ [NiCl₂(dtbpf)]^{9c} and [PdCl₂(dtbpf)]^{9c} were prepared according to the literature methods. Dichloromethane (CH₂Cl₂) and diethyl ether (Et₂O) were purified under Ar using a Solv-tek purification system similar to one previously described.¹¹ Chloroform (CHCl₃) and methanol were degassed prior to use. ³¹P{¹H} and ¹H NMR spectra were recorded using a JEOL Eclipse 400 FT-NMR spectrometer. An external reference of 85% H₃PO₄ was used for the ³¹P{¹H} spectra, while TMS was used as an internal reference for the ¹H NMR. Elemental analysis was performed by Quantitative Technologies, Inc. UV–vis experiments were conducted on a Beckman DU-65 spectrophotometer, and data were transferred to a computer and analyzed using IGOR Pro software. All experimental readings were performed using the same quartz cuvette, and CH₂Cl₂ was used as the solvent. The spectrophotometer was blanked using CH₂Cl₂ and calibrated prior to experimental procedures.

Preparation of [PtCl₂(dtbpf)]. PtCl₂(C₆H₅CN)₂ (0.0798 g, 0.169 mmol) and dtbpf (0.0806 g, 0.170 mmol) were dissolved in 20 mL of CH₂Cl₂ and stirred for 5.75 h. The volume of the solvent was then reduced to approximately 5 mL. Diethyl ether was added to the solution until a precipitate formed. This solution was filtered, and the filtrate was stripped of solvent and washed with 10 mL of hexanes. The remaining solid was subsequently washed three times with 10 mL of diethyl ether and dried to give [PtCl₂(dtbpf)] as a brownish-yellow solid (0.0267 g, 21%). Anal. Calcd for C₂₆H₄₄Cl₂FeP₂Pt: C, 42.18; H, 5.99. Found: C, 41.78; H, 5.94. ³¹P{¹H}NMR (CDCl₃): δ (ppm) 35.7 (s, ¹J_{P–Pt} = 3850 Hz). ¹H NMR (CDCl₃): δ (ppm) 4.59 (s, 4H, C₅H₄), 4.42 (s, 4H, C₅H₄), 1.8–1.2 (m, 36H, CH₃).

Preparation of [Au₂Cl₂(dtbpf)]. HAuCl₄·H₂O (0.200 g, 0.559 mmol) was dissolved in a mixture of 8.0 mL of methanol and 1.5 mL of water, and the solution was cooled to 0 °C. A solution of 2,2'-thiodiethanol (0.7 mL, 7.0 mmol) in 1.5 mL of methanol was added, and the resulting mixture was stirred for 15 min. In a separate flask, dtbpf (0.1045 g, 0.2203 mmol) was dissolved in 4 mL of chloroform and then added to the mixture. The resulting solution was stirred for 21 h, and a yellow precipitate formed. The solution was filtered, and the solid was washed twice with methanol to give [Au₂Cl₂(dtbpf)] as a yellow solid (0.0705 g, 34%). Anal. Calcd for C₂₆H₄₄Au₂Cl₂FeP₂: C, 33.25; H, 4.72. Found: C, 33.08; H, 4.59. ³¹P{¹H} (CDCl₃): δ 68.9 (s). ¹H NMR (CDCl₃): δ 4.84 (s, 4H, C₅H₄), 4.53 (m, 4H, C₅H₄), 1.39 (d, ³J_{H–P} = 15.4 Hz, 36H, CH₃).

Preparation of dtbpfS₂. A mixture of dtbpf (0.1039 g, 0.219 mmol) and sulfur (0.0140 g, 0.438 mmol) was dissolved in CHCl₃ (10 mL). The resulting red solution was refluxed with stirring for 3 h, during which time the solution turned a lighter, amber-red color. The solution was then allowed to cool to room temperature and filtered, and then the filtrate was reduced to approximately 5 mL

(10) Connelly, N. G.; Geiger, W. E. *Chem. Rev.* **1996**, *96*, 877.

(11) Pangborn, A. B.; Giardello, M. A.; Grubbs, R. H.; Rosen, R. K.; Timmers, F. J. *Organometallics* **1996**, *15*, 1518.

in vacuo. Methanol (15 mL) was added, and the resulting orange solution was placed in a freezer for 18 h, during which time an orange precipitate formed. The solid was collected by filtration and dried under vacuum, giving an orange solid (0.0072 g, 61%). Anal. Calcd for $C_{26}H_{44}FeP_2Se_2$: C, 57.98; H, 8.24. Found: C, 57.64; H, 7.98. $^{31}P\{^1H\}$ NMR ($CDCl_3$): δ (ppm) 77.78 (s). 1H NMR ($CDCl_3$): δ (ppm) 4.81 (br s, 4H, C_5H_4), 4.56 (br s, 4H, C_5H_4), 1.34 (d, $^3J_{H-P} = 15.0$ Hz, 36H, $-CH_3$).

Preparation of dtbpfSe₂. A mixture of dtbpf (0.4965 g, 1.05 mmol) and selenium (0.1651 g, 2.09 mmol) was dissolved in $CHCl_3$ (50 mL). The resulting amber-red solution was refluxed with stirring for 3 h, during which time the solution lightened in color slightly. The reaction cooled to room temperature and was reduced to approximately 5 mL in vacuo, and then methanol (30 mL) was added. The resulting orange solution was placed in a freezer for 18 h, during which time an orange precipitate formed. The solid was collected by filtration and dried under vacuum, giving an orange solid (0.5323 g, 81%). Crystals for X-ray analysis were prepared by vapor diffusion of Et_2O into a solution of dtbpfSe₂ in minimal CH_2Cl_2 in a freezer. Anal. Calcd for $C_{26}H_{44}FeP_2Se_2$: C, 49.38; H, 7.01. Found: C, 49.32; H, 6.90. $^{31}P\{^1H\}$ NMR ($CDCl_3$): δ (ppm) 74.76 (s, $^1J_{P-Se} = 700$ Hz). 1H NMR ($CDCl_3$): δ (ppm) 4.88 (br s, 4H, C_5H_4), 4.60 (br s, 4H, C_5H_4), 1.37 (d, $^3J_{H-P} = 15.8$ Hz, 36H, $-CH_3$). UV-vis (CH_2Cl_2 ; λ_{max} (nm) (ϵ , 1.0 cm⁻¹ M⁻¹): 377 (133).

Preparation of SeP(tBu)₂(2-biphenyl). A mixture of P(tBu)₂(2-biphenyl) (0.5633 g, 1.89 mmol) and selenium (0.1494 g, 1.89 mmol) was dissolved in $CHCl_3$ (50 mL). The resulting colorless solution was refluxed with stirring for 18 h, then allowed to cool. The solution was filtered and reduced to approximately 10 mL in vacuo. Methanol (30 mL) was added, and the volume of the solution was reduced to 10 mL in vacuo, at which point a white precipitate formed. The solid was collected by filtration, washed with cold methanol (5 mL), and dried under vacuum, giving SeP(tBu)₂(2-biphenyl) as a white solid (0.2676 g, 38%). Anal. Calcd for $C_{20}H_{27}PSe$: C, 63.66; H, 7.21. Found: C, 63.58; H, 7.22. $^{31}P\{^1H\}$ NMR ($CDCl_3$): δ (ppm) 71.76 (s, $^1J_{P-Se} = 742$ Hz). 1H NMR ($CDCl_3$): δ (ppm) 7.96 (m, 1H, biphenyl), 7.5–7.1 (m, 8H, biphenyl), 1.37 (d, $^3J_{H-P} = 20.0$ Hz, $-CH_3$).

Preparation of [dtbpfSe₂][BF₄]₂. A solution of acetylferrocene tetrafluoroborate (0.1480 g, 0.470 mmol) in CH_2Cl_2 (15 mL) was added to a solution of dtbpfSe₂ (0.1489 g, 0.235 mmol) in CH_2Cl_2 (10 mL). The resulting dark red-orange solution was stirred for 30 min. Et_2O (40 mL) was added to the stirred reaction mixture, yielding an orange solution and a brown precipitate. The solution was filtered, and the precipitate was collected and dried under vacuum, giving an air-sensitive, tan solid (0.0893 g, 94%). Crystals of [dtbpfSe₂][BF₄]₂ for X-ray analysis were prepared by layering Et_2O on top of a concentrated solution of [dtbpfSe₂][BF₄]₂ in CH_2Cl_2 and allowing the two solvents to slowly mix at room temperature. Anal. Calcd for $C_{26}H_{44}B_2F_8FeP_2Se_2 \cdot 1/2CH_2Cl_2$: C, 37.52; H, 5.35. Found: C, 37.38; H, 5.38. $^{31}P\{^1H\}$ NMR (CD_2Cl_2): δ (ppm) 85.09 (s, $^1J_{P-Se} = 450$ Hz). 1H NMR (CD_2Cl_2): δ (ppm) 5.31 (br s, 8H, C_5H_4), 1.84 (d, $^3J_{H-P} = 16.5$ Hz, $-CH_3$), 1.58 (d, $^3J_{H-P} = 19.1$ Hz, $-CH_3$). UV-vis (CH_2Cl_2 ; λ_{max} (nm) (ϵ , 1.0 cm⁻¹ M⁻¹): 346 (647).

Electrochemical Procedures. Cyclic voltammetric, chronoamperometric, and linear scan voltammetric experiments were conducted at ambient temperature (22 ± 1 °C) with the exception of dtbpf, which was conducted at 20, 10, 0, and -10 °C using a jacketed cell connected to a constant-temperature circulating bath (± 0.1 °C). Experiments were conducted using a PAR Model 263A potentiostat/galvanostat. All scans were performed under an argon atmosphere using 0.1 M tetrabutylammonium hexafluorophosphate ([NBu₄][PF₆]) as the supporting electrolyte and CH_2Cl_2 as the solvent, with the exception of the cyclic voltammograms of dtbpfSe₂ used for simulation, in which case the concentration of the

Table 1. Crystal Data and Structure Analysis Results

	dtbpfSe ₂	[dtbpfSe ₂][BF ₄] ₂ ·CH ₂ Cl ₂
formula	C ₂₆ H ₄₄ FeP ₂ Se ₂	C ₂₇ H ₄₆ B ₂ Cl ₂ F ₈ FeP ₂ Se ₂
fw	632.32	890.87
cryst syst	monoclinic	orthorhombic
space group	<i>P</i> 2 ₁ / <i>c</i>	<i>P</i> 2 ₁ 2 ₁ 2 ₁
<i>a</i> , Å	14.9114(11)	12.0758(13)
<i>b</i> , Å	14.0870(11)	15.8867(17)
<i>c</i> , Å	14.9432(11)	18.513(2)
α , deg	90	90
β , deg	117.7890(10)	90
γ , deg	90	90
<i>V</i> , Å ³	2410.6(4)	3551.7(7)
<i>Z</i>	4	4
cryst size, mm	0.30 × 0.15 × 0.15	0.20 × 0.20 × 0.20
cryst color	orange	yellow-orange
radiation; λ , Å	0.71073	0.71073
temp, K	100(2)	213(2)
θ range, deg	1.54–27.54	1.69–28.12
data collected		
<i>h</i>	−19 to +18	−15 to +15
<i>k</i>	−18 to +18	−21 to +20
<i>l</i>	−19 to +19	−24 to +22
no. of data collected	23 701	26 327
no. of unique data	6295	8166
absorp corr	SADABS	SADABS
final <i>R</i> indices (obsd data)		
<i>R</i> 1	0.0247	0.0347
w <i>R</i> 2	0.0612	0.0897
goodness of fit	1.027	1.072

supporting electrolyte was 0.5 M. Analyte concentrations were 1.0 mM, with the exception of dtbpf, which was studied at 0.50, 1.0, and 2.0 mM. Glassy carbon (1.5 mm disk) was used as the working electrode. The glassy carbon electrode was polished with two diamond pastes, first 1.0 μ m and then 0.25 μ m, and rinsed with CH_2Cl_2 prior to use. The experimental reference electrode was Ag/AgCl, separated by a fine frit from the solution, and the counter electrode was a platinum wire. FcH or Fc* was used as an internal standard depending on the potential of the compound being studied.¹² Cyclic voltammograms were recorded using PowerSuite software and were performed at scan rates of 50 mV/s, and from 100 to 1000 mV/s in 100 mV/s increments. Digital simulations were performed using DigiElch version 2.0.¹³

Bulk electrolyses were performed under argon using a CH Instruments Model 630B electrochemical analyzer. The working and auxiliary electrodes were platinum mesh baskets that were in compartments separated by a fine glass frit. The Ag/AgCl reference electrode was in the same compartment as the working electrode, but was also separated by a fine glass frit. A 1.5 mm glassy carbon electrode was used to obtain the cyclic voltammogram after the bulk electrolysis. The solvent was CH_2Cl_2 , and the supporting electrolyte was 0.1 M [NBu₄][PF₆]. The analyte concentration was 5.0 mM, and the temperature was 22 ± 1 °C.

Crystal Structure of dtbpfSe₂. Crystals were mounted on a CryoLoop with Paratone-N oil and immediately placed under a stream of N₂ on a Bruker SMART APEX CCD system. Data were collected at -173 °C with Mo K α radiation and corrected for absorption using the SADABS program (Table 1).¹⁴ The structure was solved from a Patterson difference map, developed by successive difference Fourier syntheses, and refined by full matrix

(12) When Fc* was used as the standard, the potentials were referenced to FcH by subtracting 0.55 V. Camire, N.; Mueller-Westerhoff, U. T.; Geiger, W. E. *J. Organomet. Chem.* **2001**, 637–639, 823.

(13) (a) Rudolph, M. *J. Electroanal. Chem.* **2003**, 543, 23. (b) Rudolph, M. *J. Electroanal. Chem.* **2004**, 571, 289. (c) Rudolph, M. *J. Electroanal. Chem.* **2003**, 558, 171. (d) Rudolph, M. *J. Comput. Chem.* **2005**, 26, 619. (e) Rudolph, M. *J. Comput. Chem.* **2005**, 26, 633. (f) Rudolph, M. *J. Comput. Chem.* **2005**, 26, 1193.

(14) Sheldrick, G. M. *SADABS* (2.01), Bruker/Siemens Area Detector Absorption Correction Program; Bruker AXS: Madison, WI, 1998.

least squares on all F^2 data. All non-hydrogen atoms were refined as being anisotropic, and hydrogen atoms were placed in calculated positions with temperature factors fixed at 1.2 or 1.5 times the equivalent isotropic U of the carbon atoms to which they were bonded.

Crystal Structure of [dtbpfSe₂][BF₄]₂. Crystals were mounted on a CryoLoop with Paratone-N oil and immediately placed under a stream of N₂ on a Bruker SMART APEX CCD system. Data were collected at -60 °C with Mo K α radiation and corrected for absorption using the SADABS program (Table 1).¹⁴ The space group was unambiguously assigned from systematic absences in the diffraction data. The structure was solved by direct methods. All non-hydrogen atoms were refined with anisotropic thermal parameters, and all hydrogen atoms were treated as idealized contributions.

Computational Details. The calculations were performed using the Spartan '04 version 1.0.3 package.¹⁵ Density functional theory (DFT) methods at the B3LYP/6-31G* level were used. Single-point energies were calculated from the crystal structures of dtbpfSe₂, [dtbpfSe₂]²⁺, dippfS₂,¹⁶ and dippfSe₂,¹⁶ which were imported and used without additional geometry optimization.

Results and Discussion

The oxidative electrochemistry of dtbpf was examined in CH₂Cl₂ with [NBu₄][PF₆] as the supporting electrolyte. At all temperatures and concentrations employed in this study, the oxidation of dtbpf was chemically and electrochemically reversible; the ratio of the peak currents (i_p^{ox}/i_p^{red}) was greater than 0.95, and the peak separation (ΔE_p) was approximately 83 mV; under identical conditions the ΔE_p for FcH was 91 mV. The potential at which oxidation of dtbpf occurs is 0.06 V vs FcH⁺⁰. The potential at which oxidation of 1,1'-(disubstituted)ferrocene compounds occurs has been correlated with the Hammett parameter (σ_p) for the substituents according to eq 1 ($E_L = 1/2E^0$ vs NHE).¹⁷ The value of σ_p for the -P(tBu)₂ group is 0.15,¹⁸ which, according to eq 1, would predict the potential at which oxidation of dtbpf occurs to be 0.20 V vs FcH⁺⁰. In general

$$E_L = 0.45\sigma_p + 0.36 \quad (1)$$

there is good agreement between the experimental potential and that predicted by eq 1, so it is surprising that there is such a large difference in this case.

The reversible oxidation of dtbpf is somewhat surprising, as the oxidative electrochemistry of two closely related compounds, dppf² and dippf,³ are complicated by a chemical reaction after oxidation. The reaction has been proposed to be a dimerization of the oxidized species through one of the phosphorus atoms.⁴ Since the product of the oxidation of dtbpf is stable on the cyclic voltammetric time scale, it would seem either that dtbpf⁺ does not undergo the same reaction as the products of dppf or dippf oxidation or that the reaction is significantly slower. Given that the potential at which dtbpf oxidation occurs is nearly identical to dippf (+0.05 V vs FcH⁺⁰),³ it is unlikely that the stability of dtbpf⁺ is due to electronic factors. It would seem that the bulky *tert*-butyl groups prevent the dimerization of dtbpf⁺ from occurring.

To further examine the electrochemistry of dtbpf, the anodic electrochemistry of four dtbpf metal complexes was investigated.

Table 2. Formal Potentials (V vs FcH⁰⁺),^a Potential Difference, ΔE (defined as $E^0_{\text{compd}} - E^0_{\text{dtbpf}}$), and Reversibility for dtbpf and Compounds Containing dtbpf (a scan rate of 100 mV/s was used for all data)

	E^0	ΔE	i_p^{ox}/i_p^{red}
dtbpf	0.06		0.95
[NiCl ₂ (dtbpf)]	0.35 ^b	0.29 ^d	0
[PdCl ₂ (dtbpf)]	0.47	0.41	0.99
[PtCl ₂ (dtbpf)]	0.46	0.40	1.00
[Au ₂ Cl ₂ (dtbpf)]	0.56	0.50	0.98
dtbpfS ₂	0.36	0.30	0.96
dtbpfSe ₂	0.24, -0.07 ^c	0.18 ^d	

^a Determined from the midpoint of E_p^{ox} and E_p^{red} . ^b The oxidation of this compound is chemically irreversible, and therefore this value is the E_p^{ox} and not E^0 . ^c The oxidation of this compound is electrochemically irreversible; the first value given is E_p^{ox} and the second is E_p^{red} . ^d The value ΔE is defined as $E_p^{ox} - E^0_{\text{dtbpf}}$.

Upon coordination, the potential at which oxidation of the iron center of dtbpf occurs shifts to more positive potentials. Similar to the dppf and dippf analogues, the oxidation of NiCl₂(dtbpf) is chemically irreversible, while the oxidation of the Pd and Pt analogues is chemically and electrochemically reversible.^{2,3} As with the free phosphines, the potentials at which oxidation of the dtbpf complexes occur (Table 2) are very similar to those of the analogous dippf complexes.³ The oxidation of [Au₂Cl₂(dtbpf)] is also chemically and electrochemically reversible and occurs at a potential similar to that of the dippf analogue. There is a gold atom bonded to each phosphorus in [Au₂Cl₂(dtbpf)], so eq 1 can be used to estimate the Hammett parameter for the -P(tBu)₂AuCl group as 0.56.

In addition to the metal complexes, we have been interested in the electrochemistry of the phosphine chalcogenides of dppf and dippf, in particular the oxidation of the diselenides. Unlike the chemically and electrochemically reversible oxidation seen for the dioxides and disulfides, the oxidative electrochemistry of the diselenides of dppf and dippf as well as that of dppfOSe was considered to be an irreversible anodic wave and a cathodic wave due to a follow-up product.⁶ It was presumed that the reaction that occurs upon oxidation was due to the presence of the selenium. However, since the products of oxidation of the parent phosphines undergo a reaction, some participation from the iron center and/or the phosphorus cannot be excluded. To eliminate participation of the iron and/or phosphorus, the selenide of a phosphine with a chemically and electrochemically reversible oxidation, such as dtbpf, must be examined.

The compounds dtbpfS₂ and dtbpfSe₂ were prepared by reacting dtbpf with the appropriate chalcogenide in refluxing CHCl₃. The ³¹P signal for dtbpfS₂ and dtbpfSe₂ was shifted downfield from that of dtbpf. The X-ray structure of dtbpfSe₂ was determined (Figure 1), and select bond lengths and angles are presented in Table 3. The structure adopted by dtbpfSe₂ is anticlinal in which the C₅ rings are staggered.¹⁹ The average P-Se distance in dtbpfSe₂ is similar to the average P-Se distances reported for dppfSe₂²⁰ and dippfSe₂,¹⁶ which are 2.102 and 2.121 Å, respectively.

Once prepared, the oxidative electrochemistries of dtbpfS₂ and dtbpfSe₂ were examined. The oxidation of dtbpfS₂ is chemically and electrochemically reversible and occurs at a more positive potential than that of dtbpf. Based on eq 1, the Hammett parameter (σ_p) for the -P(S)tBu₂ group can be estimated and

(15) *Spartan '04*; Wavefunction, Inc.: Irvine, CA.

(16) Necas, M.; Beran, M.; Woollins, J. D.; Novosad, J. *Polyhedron* **2001**, *20*, 741.

(17) Lu, S.; Strelets, V. V.; Ryan, M. F.; Pietro, W. J.; Lever, A. B. P. *Inorg. Chem.* **1996**, *35*, 1013.

(18) Hansch, C.; Leo, A.; Taft, R. W. *Chem. Rev.* **1991**, *91*, 165.

(19) (a) Gan, K.-S.; Hor, T. S. A. In *Ferrocenes. From Homogeneous Catalysis to Material Science*; Togni, A., Hayashi, T., Eds.; VCH: New York, 1995; p 3. (b) Bandoli, G.; Dolmella, A. *Coord. Chem. Rev.* **2000**, *209*, 161.

(20) Pilloni, G.; Longato, B.; Bandoli, G.; Corain, B. *J. Chem. Soc., Dalton Trans.* **1997**, 819.

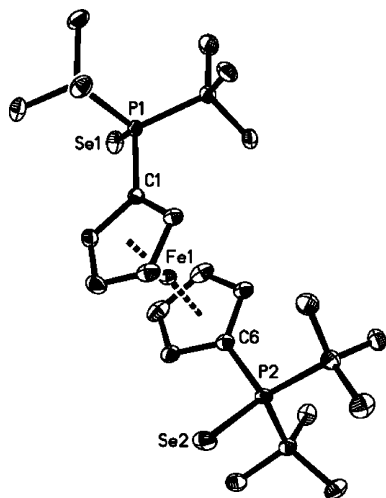


Figure 1. Perspective view of dtbpfSe₂ with 30% ellipsoids. H atoms are omitted for clarity.

Table 3. Select Bond Lengths (Å) and Angles (deg) for dtbpfSe₂

Lengths			
P(1)–Se(1)	2.1194(5)	P(2)–Se(2)	2.1200(5)
Fe–C _{Cp} (av)	2.049	P–C _{Cp} (av)	1.810
avg. δ _p ^a	–0.268		
Angles			
X _A –Fe–X _B ^b	174.92	P–Fe–P	152.47
τ ^c	138.08	θ ^d	6.29
C _{Cp} –P–Se (av)	111.14		

^a Deviation of the P atom from the C₅ plane; a positive value means the P is closer to the Fe. ^b Centroid–Fe–Centroid. ^c The torsion angle C_A–X_A–X_B–C_B where C is the carbon atom bonded to phosphorus and X is the centroid. ^d The dihedral angle between the two C₅ rings.

the value of σ_p is 0.33. Unlike the sulfide, the oxidation of dtbpfSe₂ is more complicated (Figure 2). The cyclic voltammograms of dppfSe₂, dipfSe₂, and dppfOSe are similar to that of dtbpfSe₂ and were described as an irreversible oxidation with a reduction due to a follow-up product.⁶ Since similar reactivity is not seen in the sulfide, it would seem that the presence of the Se is important to the reactivity of the oxidation product.

The oxidative electrochemistry of Fc₃P=Se is also similar to that of dtbpfSe₂.²¹ To determine whether a ferrocenyl group bonded to the phosphine selenide is necessary to observe this type of behavior, the anodic electrochemistry of (tBu)₂(2-biphenyl)P was examined. The oxidation is chemically irreversible, and the potential at which oxidation occurs is +0.40 V vs FcH^{+/0}. The oxidation of (tBu)₂(2-biphenyl)P=Se displays an anodic wave at +0.17 V vs FcH^{+/0} and a cathodic wave at –0.25 V vs FcH^{+/0}. This suggests that the anodic electrochemistry of phosphine selenides is similar regardless of the presence of a ferrocenyl group on the phosphorus.

To further examine the nature of the product of oxidation of dtbpfSe₂, chemical oxidation of dtbpfSe₂ with acetylferrocenium tetrafluoroborate was performed. Two equivalents of oxidant per equivalent of dtbpfSe₂ were consumed in this reaction. The ³¹P chemical shift is approximately 10 ppm downfield of the shift of dtbpfSe₂. A small downfield shift, approximately 6 ppm, was also noted in the ³¹P NMR of [(Me₂N)₃P–Se–Se–P(NMe₂)₃][Bi₂Cl₈] as compared to (Me₂N)₃P=Se.²² The struc-

ture of the dtbpfSe₂ oxidation product was determined to be [dtbpfSe₂][BF₄]₂ (Figure 3) in which a Se–Se bond has formed. Select bond lengths and distances for [dtbpfSe₂][BF₄]₂ are presented in Table 4.

The difference in the oxidation of dtbpfS₂ and dtbpfSe₂ was further examined by performing calculations. It is somewhat surprising that formation of a bond between the chalcogenide atoms occurs for the diselenide and not the disulfide, as the S–S bond is expected to be stronger than the Se–Se bond.²³ In addition, the oxidation of Ph₃P=S has been shown to generate Ph₃P–S–S–PPh₃²⁺.²⁴ The difference in reactivity between dtbpfS₂ and dtbpfSe₂ could be due to the greater polarizability of the P–Se bond as compared to the P–S bond as well as the decrease in the π -bond order from P–S to P–Se²⁵ or the presence of the ferrocene backbone. While the structure of dtbpfS₂ has not been determined, the structures of the electrochemically⁶ similar compounds, dipfS₂ and dipfSe₂, have been reported.¹⁶ These structures were used to perform calculations from which the HOMOs could be examined. The HOMOs of dipfS₂ and dipfSe₂ show significant contribution from a chalcogenide p-orbital (Figure 4). However, the HOMO of dipfS₂ also shows contribution from a d-orbital on iron. This suggests that oxidation of dipfS₂ either occurs at the iron center or initially occurs at sulfur but is quickly followed by an intramolecular electron transfer from the iron. The lack of participation of an iron d-orbital in the HOMO of dipfSe₂ suggests that oxidation occurs at a selenium atom. The calculations also indicate that the energy of the HOMO of dipfS₂ is –5.54 eV, which is 0.33 eV lower in energy than the HOMO of dipfSe₂ (–5.21 eV). This suggests that the potential at which oxidation occurs should be 0.16 V more positive than that of dipfSe₂. This is in excellent agreement with the experimental value of 0.17 V, which is the difference between the *E*⁰ of dipfS₂ (0.38 V) and the *E*_p^{ox} (the correct representation of what was described as an irreversible oxidation) of dipfSe₂ (0.21 V).⁶

The structure of [dtbpfSe₂][BF₄]₂ is synclinal eclipsed, although the angle τ is significantly less than the ideal angle of 72° for this structure.¹⁹ The P–Se distance in [dtbpfSe₂][BF₄]₂ is significantly longer than the corresponding distance in dtbpfSe₂, suggesting that a P–Se single bond exists in [dtbpfSe₂][BF₄]₂. The related compound, [(Me₂N)₃P–Se–Se–P(NMe₂)₃][Bi₂Cl₈], was prepared by the oxidation of (Me₂N)₃P=Se by BiCl₃.²² The average P–Se length in [dtbpfSe₂][BF₄]₂ is similar to the average P–Se length of 2.230 Å found for [(Me₂N)₃P–Se–Se–P(NMe₂)₃][Bi₂Cl₈].²² In addition, the Se–Se bond length in [(Me₂N)₃P–Se–Se–P(NMe₂)₃][Bi₂Cl₈], 2.309(5) Å,²² is similar to the corresponding distance in [dtbpfSe₂][BF₄]₂. The P–Se–Se–P torsion angle is significantly smaller in [dtbpfSe₂][BF₄]₂ than in [(Me₂N)₃P–Se–Se–P(NMe₂)₃][Bi₂Cl₈] due to the ferrocenyl backbone in [dtbpfSe₂][BF₄]₂.

In addition to the bonding in the P–Se–Se–P linkage, the location of the positive charge is also of interest. The average Fe–C bond length in [dtbpfSe₂][BF₄]₂ is slightly longer than that of dtbpfSe₂. There is a significant lengthening of the Fe–C bond lengths on going from ferrocene to ferrocenium;²⁶ therefore, it would seem that the iron center in [dtbpfSe₂][BF₄]₂

(23) McDonough, J. E.; Weir, J. J.; Carlson, M. J.; Hoff, C. D.; Kryatova, O. P.; Rybak-Akimova, E. V.; Clough, C. R.; Cummins, C. C. *Inorg. Chem.* **2005**, *44*, 3127.

(24) Blankespoor, R. L.; Doyle, M. P.; Smith, D. J.; Van Dyke, D. A.; Waldyke, M. J. *J. Org. Chem.* **1983**, *48*, 1176.

(25) (a) Shagidullin, R. R.; Vandyukova, I. I.; Nuretdinov, I. A. *Izv. Akad. Nauk SSSR, Ser. Khim.* **1978**, 1407. (b) Sandblom, N.; Ziegler, T.; Chivers, T. *Can. J. Chem.* **1996**, *74*, 2363.

(21) Barriere, F.; Kirss, R. U.; Geiger, W. E. *Organometallics* **2005**, *24*, 48.

(22) Willey, G. R.; Barras, J. R.; Rudd, M. D.; Drew, M. G. B. *J. Chem. Soc., Dalton Trans.* **1994**, 3025.

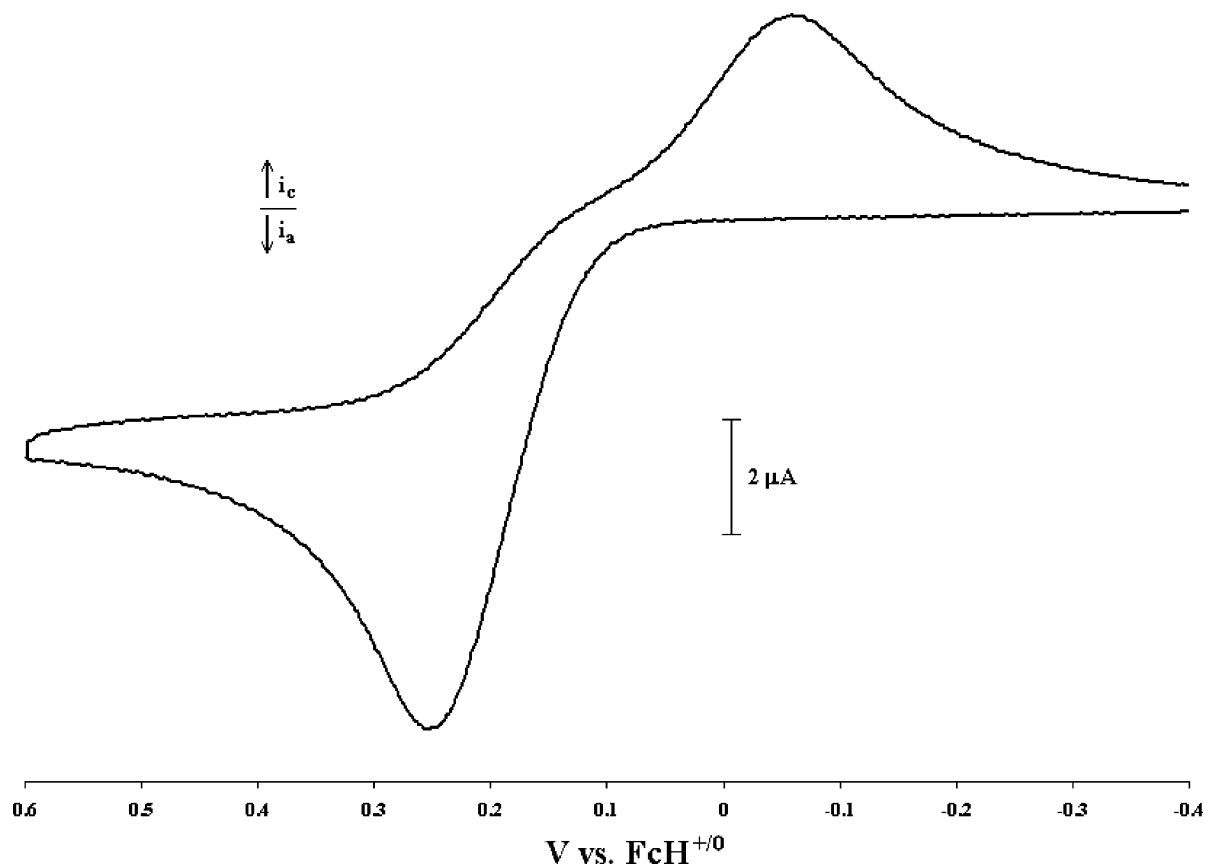


Figure 2. CV for the oxidation of 1.0 mM dtbpfSe₂ in CH₂Cl₂/0.1M [NBu₄][PF₆] at a glassy carbon electrode and a scan rate of 100 mV/s.

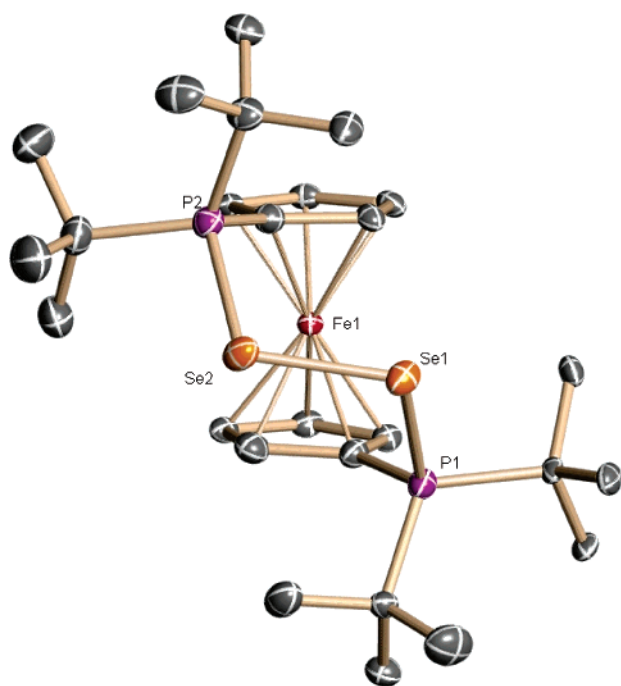


Figure 3. Perspective view of [dtbpfSe₂][BF₄]₂ with 30% ellipsoids. H atoms are omitted for clarity.

is formally in the +2 oxidation state. The average C_{Cp}–P distance in dtbpfSe₂ is 0.014 Å longer than the analogous distance in [dtbpfSe₂][BF₄]₂. In addition, the carbon–carbon

Table 4. Select Bond Lengths (Å) and Angles (deg) for [dtbpfSe₂][BF₄]₂

Lengths			
P(1)–Se(1)	2.2788(9)	P(2)–Se(2)	2.2718(9)
Fe–C _{Cp} (av)	2.056	P–C _{Cp} (av)	1.796
Se(1)–Se(2)	2.3330(5)	av δ _P ^a	–0.150
Angles			
X _A –Fe–X _B ^b	175.15	P–Fe–P	88.37
τ ^c	65.03	θ ^d	2.98
C _{Cp} –P–Se (av)	112.31	P(1)–Se(1)–Se(2)–P(2)	–96.19

^a Deviation of the P atom from the C₅ plane; a positive value means the P is closer to the Fe. ^b Centroid–Fe–Centroid. ^c The torsion angle C_A–X_A–X_B–C_B where C is the carbon atom bonded to phosphorus and X is the centroid. ^d The dihedral angle between the two C₅ rings.

bond lengths for the C₅H₄ carbon bound directly to phosphorus are approximately 0.02 Å longer than the other carbon–carbon distances in the C₅H₄ ring. The shorter P–C bond and differences in C–C bond lengths in [dtbpfSe₂][BF₄]₂ suggest increased interaction with the π-system of the C₅H₄ rings and a resonance structure in which the cation is localized on the ylide phosphorus (Figure 5). Similar structural features have been examined in a series of phosphinobenzo[*c*]phospholides.²⁷

To determine if [dtbpfSe₂][BF₄]₂ was formed during cyclic voltammetric experiments and the nature of the follow-up reduction, a more complete electrochemical analysis was performed. Bulk anodic electrolysis confirmed that the oxidation was a two-electron process ($n_{app} = 1.9 e^-$, $E_{app} = 0.9$ V vs Ag/AgCl based on a cyclic voltammogram of the bulk solution, $T = 22 \pm 1$ °C, color change from orange to faint yellow-orange). A sample of the solution was removed and a ³¹P{¹H} spectrum obtained. In addition to the large peak at –143.9 ppm

(26) (a) Mammano, N. J.; Zalkin, A.; Landers, A.; Rheingold, A. L. *Inorg. Chem.* **1977**, *16*, 297. (b) Churchill, M. R.; Landers, A. G.; Rheingold, A. L. *Inorg. Chem.* **1981**, *20*, 849. (c) Paulus, E. F.; Schäfer, L. *J. Organomet. Chem.* **1978**, *144*, 205.

(27) Haep, S.; Szarvas, L.; Nieger, M.; Gudat, D. *Eur. J. Inorg. Chem.* **2001**, 2763.

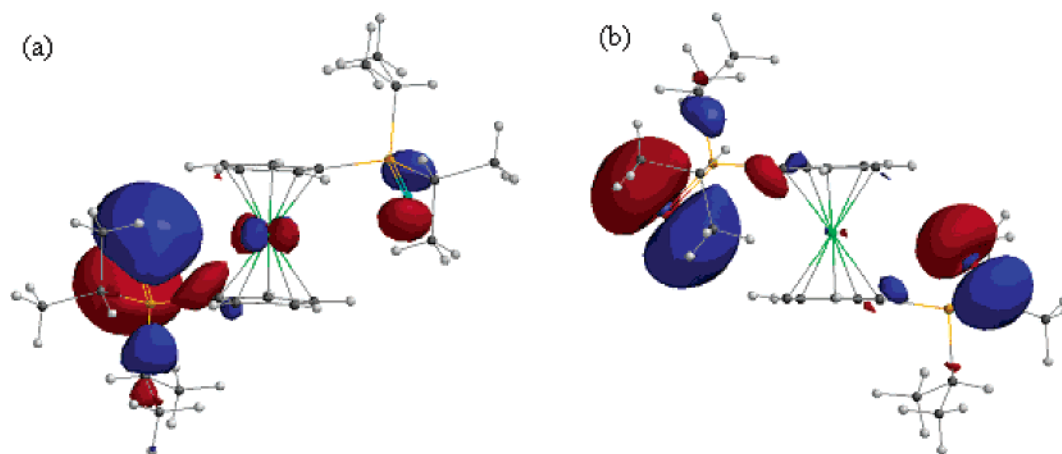


Figure 4. Molecular orbital surfaces showing the HOMO of dippfS₂ (a) and dippfSe₂ (b).

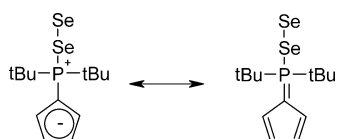


Figure 5. Resonance structures of [dtbpfSe₂]²⁺. The Fe and other C₅ ring are omitted for clarity.

for the PF₆[−] of the supporting electrolyte, a peak at 85.2 ppm was observed, suggesting that the Se–Se bonded species, [dtbpfSe₂]²⁺, was formed during the electrolysis. Back-reduction of the solution at 0.2 V vs Ag/AgCl regenerated dtbpfSe₂ on the basis of a cyclic voltammogram and ³¹P{¹H} NMR of the resulting solution. This would suggest that the electrochemical process is either a 2 e[−] process or two 1 e[−] processes. Bulk anodic electrolysis of dtbpfS₂ showed that the oxidation was a one-electron process ($n_{\text{app}} = 1.0 e^-$, $E_{\text{app}} = 1.0 \text{ V vs Ag/AgCl}$ based on a cyclic voltammogram of the bulk solution, $T = 22 \pm 1 \text{ }^\circ\text{C}$, color change from orange to green-yellow), suggesting that oxidation of dtbpfS₂ occurs at the iron center as opposed to sulfur.

To explore the mechanism of electron transfer, the experimental cyclic voltammograms were compared to theoretical ones. The cyclic voltammograms used for comparison were run at higher concentration of supporting electrolyte in order to minimize resistance in the solution. Assuming a 2 e[−] process, the diffusion coefficient for dtbpfSe₂ at $22 \pm 1 \text{ }^\circ\text{C}$ is $7.0 \times 10^{-6} \text{ cm}^2/\text{s}$ based on chronoamperometric data. Simulation of the voltammetric response of dtbpfSe₂ as two separate one-electron processes (an EE mechanism)²⁸ gave good agreement with the experimental data (Figure 6). It is possible that there is a chemical step that occurs between the electron transfer steps (an ECE mechanism);²⁸ however, there are no changes in the voltammetric features at scan rates from 50 to 1000 mV/s, suggesting that there is not a chemical step occurring between the electron transfer steps. In this simulation, the second couple (dtbpfSe⁺/dtbpfSe₂²⁺) occurs at a less positive potential than the first couple (dtbpfSe₂/dtbpfSe₂⁺) (Table 5). In addition, the second charge transfer is slower than the first. A similar mechanism, in which the second oxidation occurs at a potential less positive than the first but the first electron transfer is slower than the second, was proposed for the oxidation of (Fv)Rh₂(CO)₄ (Fv = C₅H₄–C₅H₄).²⁸ The oxidation of (Fv)Rh₂(CO)₄ to (Fv)Rh₂(CO)₄²⁺ also results in the formation of a Rh–Rh

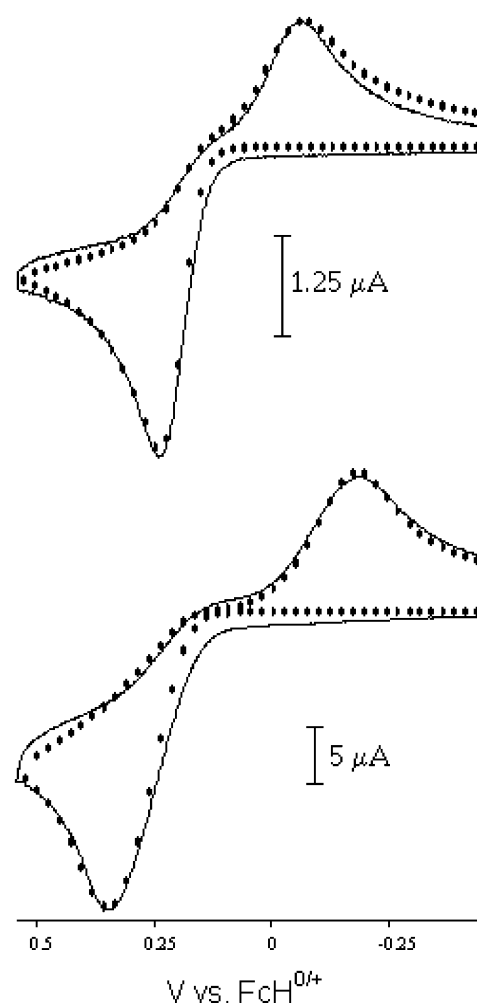


Figure 6. Cyclic Voltammograms of dtbpfSe₂ in CH₂Cl₂. Comparison of experimental data (solid lines) and simulations (circles) for an EE mechanism at 100 mV/s (top) and 1000 mV/s (bottom).

bond, the formation of which was proposed to be linked to both electron transfer steps.²⁹

Formation of the Se–Se bond in [dtbpfSe₂]²⁺ requires not only oxidation but also some structural reorganization of the complex. Using the data obtained from the simulations as well as data available in the literature, the energy of these processes

(28) Geiger, W. E. In *Laboratory Techniques in Electroanalytical Chemistry*, 2nd ed.; Kissinger, P. T., Heineman, W. R., Eds.; Marcel Dekker: New York, 1996; p 683.

(29) Chin, T. T.; Geiger, W. E.; Rheingold, A. L. *J. Am. Chem. Soc.* **1996**, *118*, 5002.

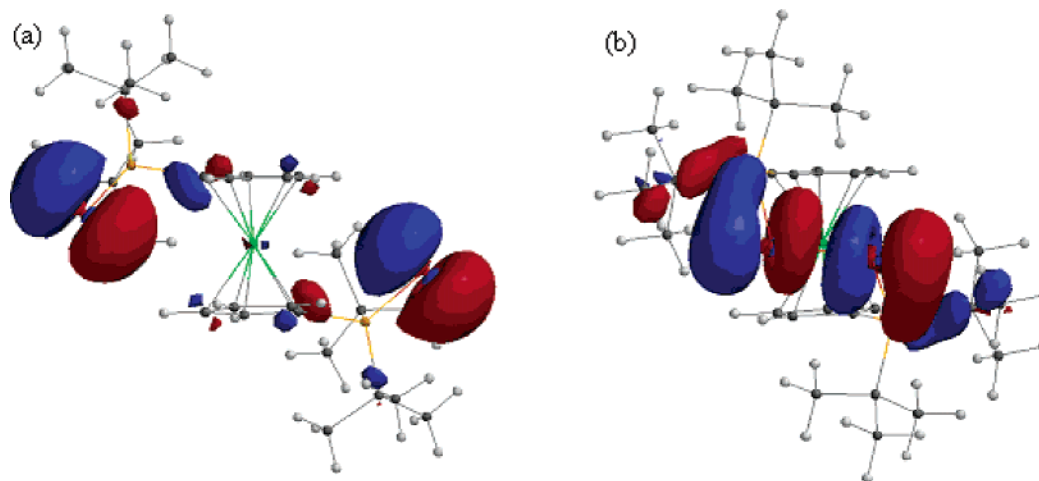


Figure 7. Molecular orbital surfaces showing the HOMO of dtbpfSe₂ (a) and the LUMO of [dtbpfSe₂]²⁺ (b).

Table 5. Average of Best Simulation Fits for the Voltammetric Parameters of dtbpfSe₂ at Glassy Carbon, *T* = 295.15 K, Potentials vs FcH^{0/+}

couple	<i>E</i> ⁰ (V)	<i>k</i> _s (cm/s)	α	Δ <i>G</i> ^{‡a}
dtbpfSe ₂ /dtbpfSe ₂ ⁺	0.23	0.012	0.5	8.0
dtbpfSe ₂ ⁺ /dtbpfSe ₂ ²⁺	0.03	0.001	0.5	9.5

^a Electron transfer activation barrier (kcal/mol) from $k_s = \kappa Z e^{-\Delta G^\ddagger/RT}$ assuming adiabatic charge transfer ($\kappa = 1$) and a collision velocity (*Z*) of 10⁴ cm/s.

can be estimated. The activation barrier, Δ*G*[‡], is the sum of the outer-sphere contribution, Δ*G*[‡]_{OS}, and the inner-sphere contribution, Δ*G*[‡]_{IS}.²⁹ The term Δ*G*[‡]_{OS} is related to the solvent and can be estimated as 4.2 kcal/mol for CH₂Cl₂.³⁰ The term Δ*G*[‡]_{IS} is equal to λ_{IS}/4 where λ_{IS} is related to the energy of C₅ ring rotation and the formation of the Se–Se bond.²⁹ The barrier to rotation of a C₅ ring in a ferrocenyl system can be approximated as 2.0 kcal/mol.³¹ Although the Se–Se bond dissociation energy for a P⁺–Se–Se–P⁺ system is not known, an estimate of 46 kcal/mol based on R–Se–Se–R (R = H, Me, or Ph) can be used.³² These approximations give a value of 12 kcal/mol for Δ*G*[‡]_{IS} and, when combine with Δ*G*[‡]_{OS}, estimate the activation barrier as approximately 16 kcal/mol. On the basis of the simulations, the sum of the Δ*G*[‡] values for the individual electron transfer steps is 17.5 kcal/mol, which is in good agreement with the estimated value from Δ*G*[‡]_{OS} and Δ*G*[‡]_{IS}. The individual Δ*G*[‡] values for each electron transfer step are both significantly less than that of the overall process, suggesting that formation of the Se–Se bond is associated with both steps of the mechanism. However, the significantly slower second step does suggest that there is a larger structural change associated with that step.

Calculations show that the HOMO of dtbpfSe₂ is nonbonding and centered on selenium, while the LUMO of [dtbpfSe₂]²⁺ is a Se–Se σ*-orbital (Figure 7). The LUMO of [dtbpfSe₂]²⁺ was calculated to be 3.42 eV lower in energy than the HOMO of dtbpfSe₂. This suggests a much larger difference than the 0.31 V observed for potentials at which oxidation of dtbpfSe₂ and the reduction of [dtbpfSe₂]²⁺ occur. However, the calculations

cannot account for molecular rearrangements or reordering of the orbitals. The LUMO of [dtbpfSe₂]²⁺ is clearly Se–Se antibonding, so the addition of two electrons to this orbital is expected to break the Se–Se bond and thereby regenerate the starting material. This is in good agreement with bulk electrolysis results.

Summary

The oxidative electrochemistry of dtbpf is chemically and electrochemically reversible, in contrast to related bis-phosphinometallobenes. Upon coordination, the oxidation of dtbpf is typically chemically and electrochemically reversible, although the potential at which oxidation occurs is more positive than that of free dtbpf. Unlike Ph₃P=Se,²⁴ the one-electron oxidation of dtbpfSe₂ is chemically and electrochemically reversible due to the presence of the ferrocene backbone. Oxidation of dtbpfSe₂ has been thoroughly studied; the oxidation of dtbpfSe₂ is best described as chemically reversible and electrochemically irreversible and with concerted electron transfer (an EE mechanism).²⁸ Presumably, the same description, as opposed to the previously suggested irreversible anodic wave and a cathodic wave due to a follow-up product, would apply to the oxidation of dppfSe₂, dppfOSe, dpprSe₂, and dippfSe₂.⁶ The Se–Se bonded species, [dtbpfSe₂]²⁺, is formed both electrochemically and by chemical oxidation. The LUMO of [dtbpfSe₂]²⁺ is Se–Se antibonding in nature, and the reduction of [dtbpfSe₂]²⁺ results in dtbpfSe₂ being re-formed. A detailed analysis of the electrochemistry indicates that the oxidation proceeds as two different one-electron processes, both of which have significant Se–Se bond forming components. This reversible formation of a diselenide bond by oxidation is of interest in the formation of Se–Se bridged peptides.³³ The intermolecular formation of Se–Se bonds from P=Se³⁴ and P–Se–H³⁵ compounds has been reported, but none of these compounds have been structurally characterized. This report includes the first structure in which there has been intramolecular formation of a diselenide by

(30) Gennett, T.; Milner, D. F.; Weaver, M. J. *J. Phys. Chem.* **1985**, *89*, 2787.

(31) Mann, B. E.; Spencer, C. M.; Taylor, B. F.; Yavari, P. *J. Chem. Soc., Dalton Trans.* **1984**, 2027.

(32) (a) Gonzales, J. M.; Musaev, D. G.; Morokuma, K. *Organometallics* **2005**, *24*, 4908. (b) McDonough, J. E.; Weir, J. J.; Carlson, M. J.; Hoff, C. D.; Kryatova, O. P.; Rybak-Akimova, E. V. Clough, C. R.; Cummins, C. C. *Inorg. Chem.* **2005**, *44*, 3127.

(33) (a) Koide, T.; Itoh, H.; Otaka, A.; Yasui, H.; Kuroda, M.; Esaki, N.; Soda, K.; Fujii, N. *Chem. Pharm. Bull.* **1993**, *41*, 502. (b) Besse, D.; Moroder, L. *J. Pept. Sci.* **1997**, *3*, 442. (c) Pegoraro, S.; Besse, D.; Fiori, S.; Rudolph-Bohner, S.; Watanabe, T. X.; Kimura, T.; Moroder, L. In *Innovation and Perspectives in Solid Phase Synthesis & Combinatorial Libraries: Peptides, Proteins and Nucleic Acids - Small Molecule Organic Chemical Diversity*; Collected Papers, 5th International Symposium; Epton, R., Ed.; Kingswinford, UK: London, 1999; pp 89–92.

(34) Krawczyk, E.; Skowronska, A.; Michalski, J. *J. Chem. Soc., Dalton Trans.* **2002**, 4471.

(35) Mielniczak, G.; Lopusinski, A. *Heteroat. Chem.* **2003**, *14*, 121.

oxidation. Additional reactivity and electrochemical studies of dtbpfSe₂, [dtbpfSe₂]²⁺, and related compounds will be reported.

Acknowledgment. F.N.B., L.E.H., W.R.M., and C.N. thank the donors of the Petroleum Research Fund, administered by the American Chemical Society, for partial funding of this research, the Kresge Foundation for the purchase of the JEOL NMR, the Academic Research Committee at Lafayette College for funding EXCEL scholars, and Professor Tina Huang of Lafayette College for use of the CH Instruments electrochemical

analyzer. C.N. would also like to thank Ken Haug of Lafayette College for his helpful discussions regarding the calculations and the reviewers for their insightful comments.

Supporting Information Available: Files in cif format for the structures of dtbpfSe₂ and [dtbpfSe₂][BF₄]₂. This material is available free of charge via the Internet at <http://pubs.acs.org>.

OM051011+